

Received August 8, 2019, accepted August 25, 2019, date of publication September 4, 2019, date of current version September 18, 2019.

Digital Object Identifier 10.1109/ACCESS.2019.2939502

# Green Internet of Things Application of a Medical Massage Robot With System Interruption

WEN SI<sup>ID 1</sup>, GAUTAM SRIVASTAVA<sup>ID 2,3</sup>, YIZHONG ZHANG<sup>4</sup>, AND LEI JIANG<sup>ID 5,6</sup>

<sup>1</sup>Department of Information and Computer Science, Shanghai Business School, Shanghai 201400, China

<sup>2</sup>Department of Mathematics and Computer Science, Brandon University, Brandon, MB R7A 6A9, Canada

<sup>3</sup>Research Center for Interneuronal Computing, China Medical University, Taichung 40402, Taiwan

<sup>4</sup>Robotics Research Centre, Nanyang Technological University, Singapore 639798

<sup>5</sup>Department of Rehabilitation, Shenzhen Longhua District Central Hospital, Shenzhen 518110, China

<sup>6</sup>Rehabilitation Department, Hannover Medical School, 30625 Hannover, Germany

Corresponding authors: Gautam Srivastava (srivastavag@brandonu.ca) and Lei Jiang (jiang.lei@mh-hannover.de)

This project was supported by the Natural Science Foundation of Shanghai (CN) (Nos. 14ZR1429800, 15ZR1430000, 18ZR1427400, and 18ZR1427500), and the Ministry of Education of the People's Republic of China (No. EIA140412).

**ABSTRACT** Safe operation control systems are the most important aspect of medical device development apart from the machine's function itself. Due to the fact that machines are used on people, how people can protect themselves from intelligent/programmed automatic or semiautomatic operating systems is an unavoidable problem. The Massage Robot application is based on its medical potential, lightweight nature and underlying Internet of Things (IoT) device properties. Massage robots are currently going into development in clinical trials. Handheld system interruption equipment and the robot's physical characteristics can help people achieve harmless use. In this paper, we systematically test the safety of a massage robot in an entirely real-world setting. This paper focusses on safe control operations in order to keep exploring the most reasonable safe operating modes and interrupt modes for medical devices, as well as the security interrupt priority.

**INDEX TERMS** Internet of Things, lightweight, medical devices, massage robots, safety, device control.

## I. INTRODUCTION

According to technological development, new automation products are increasingly used in the medical field. The Medical Massage Robot's introduction into mainstream physiotherapy can keep physiotherapists free from repeating massage actions. Moreover, it makes the massage treatment quantifiable, measurable and effortless to record the resulting data for analysis. However, a medical machine must follow a range of safety standards for not only the hardware but also the software. More importantly, a medical product must withstand real-world experience testing to determine its actual safety performance before it can be used in an actual clinic. Whatever the design criteria are, if usage in medical healthcare is the end goal, the machine must operate safely. EMMA is a massage robot as shown in Figure 2. The robot operates in an Internet of Things (IoT) environment collecting data for future analysis. This deepens the requirements for network security and patient privacy for the massage robot to function properly.

The associate editor coordinating the review of this article and approving it for publication was Jun Wu.

Safety of the equipment for people is the most important requirement for basic equipment as well. The IEC 62304 international standard delineates software safety for medical devices - the software life cycle process is a standard that specifies life cycle requirements for the development of medical software and software within medical devices. It is harmonized by the European Union (EU) [1] and the United States (US) [2] and therefore can be used as a benchmark to comply with regulatory requirements from both of these markets. The standard spells out a risk-based decision model that indicates when the use of software of unknown pedigree or provenance (SOUP) is acceptable and defines testing requirements for SOUP to support a rationale on which such software should be used [3].

The CE certification indicates conformity with health, safety, and environmental protection standards for products sold within the European Economic Area (EEA) [4]. Existing in its present form since 1985, the CE marking indicates that the manufacturer or importer claims compliance with the relevant EU legislation applicable to a product, regardless of the place of manufacture. By affixing the CE marking onto a product, a manufacturer effectively declares, at its sole

responsibility, conformity with all of the legal requirements to achieve a CE marking, which allows free movement and sale of the product throughout the European Economic Area [5].

The IoT (Internet of Things) is the network of devices: it uses the Internet, traditional telecommunications networks and other information carriers to enable all ordinary objects that can perform independent functions to realize interconnected networks [6]. The IoT can be viewed as a global infrastructure for the information society [7], enabling advanced services by interconnecting (physical and virtual) things based on existing and evolving interoperable information and communication technologies (ICT). In the current technology background, IoT medical devices represent a future development direction [8].

The EMMA Massage Robot is an IoT device that can help physiotherapists to conduct and optimize massage treatment for patients. It includes the mainframe, a robot arm, and a massage end-effector. It is designed with the complete safety standards of software and hardware, due to its design mission. This study used real-world clinical simulation tests to evaluate the safety of the EMMA Massage Robot with respect to both hardware and software; in particular, we focused on its handheld system interruption equipment module, which is held in the patient's hand to interrupt the robot action immediately in an emergency situation.

## II. RELATED WORK

The EMMA Massage Robot is used as a therapy machine: as smart equipment, most of the time it works in fully automatic or semiautomatic mode, and therefore, this mode of work determines that the patient should have the highest priority to interrupt its operation during an emergency or just because the patient desires to do so. In this situation, the handheld system interruption equipment module is designed to be held in a patient's hand, and he/she can stop the machine from running with one button anytime the patient wants [9]. The wired connection is used for its more reliable stability than the wireless one. Besides, the robotic arm strength control, movement control and emergency button control can also ensure the safe operation of robotic treatment [10], [11].

### A. MASSAGE FORCE CONTROL METHOD

High accuracy in position tracking and massage force control is required for the massage robot during the process of operation. According to the requirements of massage force control, and combined with the structural characteristics of the robot, the control method of massage force was studied in this section. When massaging, the end of the massage robot contacts with the skin surface of the human body [13]. In fact, the human skin and muscle system is a viscoelastic body, so it is necessary to solve the contradiction between the position servo of the end of the robot and the stiffness of the mechanical structure and the flexibility of the force, that is, the pliancy of the robot. The massage robot system studied in this paper was applied to the human body, and it had a high requirement for force control. In order to complete the

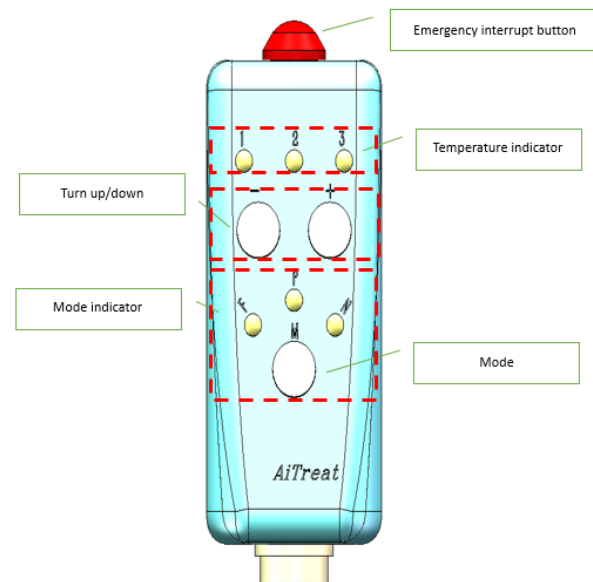


**FIGURE 1.** The handheld system interruption equipment module integrated heat source control and mechanical finger force control unit, and a block of relevant code.

massage operation, the system must have the ability of this type of pliant control. Therefore, active pliant control was developed to achieve massage force control in the paper [14].

In view of the characteristics of the active pliant control method, and considering that the control system of the massage robot of traditional Chinese medicine had high requirements for the accuracy of position and force input, the force/bit hybrid control strategy was applied in the paper, and the control modes included two types, namely, the position closed-loop mode based on massage trajectory, and the force closed-loop mode based on massage force. The specific methods are as follows:

Adopt position closed-loop mode: in the process of massage, for a certain position on the massage trajectory, the end reaches the target position through the position servo control algorithm; Switch to force closed-loop mode; calculate the position error as the input to the next position of the massage trajectory; Repeat the above steps until the simulation is completed.

### B. MIXED CONTROL MODEL OF FINGER-RUBBING MANIPULATION FORCE/POSITION

Aiming at the commonly used finger-rubbing technique, the control model was established. The massage arm was regarded as a rigid body, and the mechanical system model was simplified into a three-degrees-of-freedom Cartesian coordinate model [15] [16]. The mechanical system model of the finger-rubbing method was established through the MATLAB/Simulink toolbox, and the control system model of the finger-rubbing method was established through the Simulink toolbox. First, a model of the lead screw drive position servo control system was established, which included a lead screw drive model, PID position controller, and massage

force feedback signal collected by a pressure sensor installed on the massage hand [17]–[20].

In addition, the spring damping system model was established.

Human skin and muscle tissue were simulated to obtain the contact force between the end of the massage hand and the human body. The spring damping system model was established as shown in the following formula:

$$F(s) = \left( K + \frac{B}{S} \right) x(s)$$

where  $F(s)$  denotes the contact force between the end of the massage hand and the human body;  $x(s)$  is the position of the end of the massage hand; and  $K$  and  $B$  represent the stiffness coefficient and damping coefficient, respectively.

The force feedback servo control system model based on the contact force model of the spring damping system was established by using the PI controller as the force controller [21].

Combined with the lead screw drive position servo control system model, the force/position hybrid control model of three degrees of freedom for the finger-rubbing manipulation was finally established. The massage trajectory points included X, Y, and Z spatial coordinates and massage forces. The position and force on the trajectory were tracked [22]–[24]. After the end space position reached the target point, it was switched to force control mode. When the end reached the desired force, the force level tracking at the next point was carried out, and finally, the simulation of the control system was completed [15], [25].

According to the simulation results, the input and output trajectory of the finger-rubbing massage and the massage force of each point at the end of the robot could be obtained. The X-axis and Y-axis directions were position control, and the Z-axis direction was force-position hybrid control [26]. The position tracking error was less than 2.5 mm, and the massage force tracking error was less than 5% of the massage force, which met the design requirements.

### C. KINEMATICS ANALYSIS OF THE MASSAGE ROBOT

The main task of the kinematics analysis of the massage robot is to analyze the forward and inverse kinematics solutions of the robot module constructed by the digital platform and the massage arm, with the center point of the massage head movement platform as the output point of the end of the massage robot [27]. The configuration was composed of three perpendicular prismatic joints and four revolute joints, and the D-H method was adopted in the paper.

The kinematics model was established, and the method to solve the forward and inverse kinematics solutions was given [28]. The general formula for connecting rod transformation is as follows:

$$ii - 1T$$

$$= [c\theta_i - s\theta_i 0\alpha_{i-1} s\theta_i c\alpha_{i-1} c\theta_i c\alpha_{i-1} \\ - s\alpha_{i-1} - d_i s\alpha_{i-1} s\theta_i s\alpha_{i-1} c\theta_i s\alpha_{i-1} c\alpha_{i-1} d\alpha_{i-1} 0001]$$

The matrix of the fixed coordinate system {8} of the massage finger under the base coordinate system {0} could be obtained:

$$80T = 10T 21T \cdots 87T$$

### D. INVERSE KINEMATIC SOLUTION ESTABLISHED BY THE D-H METHOD

The configuration of the robot was composed of three coordinates and four rotation pairs, for which the characteristic was that the posture of the massage hand was completely realized by the following four rotations. In this way, the inverse kinematics solution of the robot could be obtained by using the method of pose separation. In this paper, the solidification method  $\theta_4$  was adopted to solve  $\theta_5$ ,  $\theta_6$  and  $\theta_7$  by using the terminal attitude matrix. Next,  $\theta_5$ ,  $\theta_6$  and  $\theta_7$  were used to solve  $30T$ . After obtaining  $30T$ , it was easy to solve for  $d_1$ ,  $d_2$  and  $d_3$ .

The configuration characteristics of the robot were that joints 5, 6 and 7 were perpendicular to each other. Therefore, in terms of attitude, the motion of joint 5 was equivalent to the rotation of the coordinate system {8} around  $-Y_8$ ; the motion of joint 6 was equivalent to the rotation of the coordinate system {8} around  $X_8$ ; the motion of joint 7 was equivalent to the rotation of the coordinate system {8} around  $Z_8$ . It was known that

$$80T = [x_8 80R y_8 z_8 0001]$$

$$\text{Based on } 80R = 40RRot(Y_8, -\theta_5)Rot(X_8, \theta_6)Rot(Z_8, \theta_7)$$

$$80R \cdot 40R^T = [c\theta_5 c\theta_7 - s\theta_5 s\theta_6 s\theta_7 - c\theta_7 s\theta_5 s\theta_6 \\ - c\theta_5 s\theta_7 - c\theta_6 s\theta_5 c\theta_6 s\theta_7 c\theta_6 c\theta_7 \\ - s\theta_6 c\theta_7 s\theta_5 + c\theta_5 s\theta_6 s\theta_7 c\theta_5 c\theta_7 s\theta_6 \\ - s\theta_5 s\theta_7 c\theta_5 c\theta_6]$$

$$80R \cdot 40R^T = [r_{11} r_{12} r_{13} r_{21} r_{22} r_{23} r_{31} r_{32} r_{33}]$$

If  $\cos \theta_6 \neq 0$ , each angle could be expressed as:

$$\begin{aligned} \theta_5 &= A \tan \tan 2(-r_{13}, r_{33}) \theta_6 \\ &= A \tan \tan 2(-r_{23}, \sqrt{r_{21}^2 + r_{22}^2}) \theta_7 \\ &= A \tan \tan 2(-r_{21}, r_{22}) \end{aligned}$$

If  $\theta_6 = \pm 90^\circ$ , it was singular, and there was more than one solution.

From the above,  $\theta_5$ ,  $\theta_6$  and  $\theta_7$  and the solidified  $0_4$ ,  $43T$ ,  $54T$ ,  $65T$ ,  $76T$  could be obtained.  $87T$  was the invariant. Therefore,  $30T = 80T 33T^{-1}$ . At this point,

$$30T = [x_3 30R y_3 z_3 0001]$$

It was easy to derive that:

$$d_1 = z_3 d_2 = y_3 d_3 = x_3$$

### III. SYSTEM MODEL AND DESIGN GOALS

This work attempts to describe the EMMA Massage Robot's structural features, measure the physical characteristics, and

test its specific functional performance under extreme conditions in order to ascertain the true functional performance situation.

The security design of the EMMA massage robot includes 6 main parts, meanwhile, the handheld system interruption equipment system has the first priority, and they are:

1) Handheld system interruption equipment system. Designed to stop the EMMA massage robot action in any situation with one button, and the handheld system integrated heating, which has three-level adjustments, along with intensity control.

2) Robot movement speed limit system. The movement of the robot is limited to a lower speed in order to maintain safety or leave people with enough time to react and operate it. More importantly, the movement of the robot is telecontrolled by the operator, instead of an autonomous intelligent movement solution.

3) Robot arm movement speed limit system. The robot arm movement unit can be controlled by both AI and operator telecontrol. Physical limits on the power of the device's capabilities are the main solution.

4) Robot arm forces limit system. With the same idea of robot arm movement power limitation, the forces of the robot arm, finger and pad are designed with a power limiting motor.

5) Underlying program security system. In the underlying program automated controls of mechanical transmission parts, the designed security system can ensure safety in case the software system loses function.

6) Emergency stop button basic system. The emergency stop button is the extent of the underlying program safety system, and it offers a marked big red button that is used to interrupt all actions of the massage robot, just like the function of the handheld interruption equipment button; however, the priority and logical levels of the actions are not the same inside of the EMMA hardware system, which is only used by the operator.

The speed limitation of both the robot movement and robot arm movement are in mechanical capability level, however, the precise motion control is in the software level. Taking security as the first starting point, limitation from machine movement level is more stable.

The EMMA massage robot also has an Uninterruptible Power Supply (UPS) system to prevent power supplement accidents as well. In extreme cases, the power supplement accident happens unexpectedly, the UPS will continue supply the robot running, meanwhile, the robot will stop the therapy at once and retract the robot arm back to the initial position, in order to make adequate space for the patient leaving out.

#### A. MASSAGE STRENGTH CONTROL EXPERIMENT

##### 1) EXPERIMENTAL PRINCIPLES AND METHODS

The massage force is the force that the robot exerts on the surface of the person being massaged. According to the different massage techniques and massage positions, the massage strength has corresponding characteristics. In the common

massage techniques, the fingers press, the palm kneads, and it vibrates and exerts additional massage force vertical to the massage surface. By contrast, the massage force of the rolling massage technique is the resultant force of a vertical massage surface and torque rolling along the massage surface. As for the holding technique, a pair of forces with the same size and opposite directions is applied to the massage object by placing the thumb opposite to other fingers. Therefore, the hand rubbing technique was used in the experiment to test the control accuracy of massage force.

An electronic scale with a resolution of 0.005 kg and a range of 20 kg was selected as the massage strength measurement equipment for the massage strength testing platform. The electronic scale was placed on the massage table to imitate the object being massaged. The massage robot applied the palm-rubbing technique with a given massage force. By using the electronic scale to measure the massage force, the massage force exerted by the robot was compared, and the control performance of the massage force was analyzed.

##### 2) EXPERIMENTAL PROCESS

Place the electronic scale horizontally on the massage table mat; Move the end-effector of the massage robot directly above the electronic scale, and keep the bionic finger/palm perpendicular to the horizontal plane; Set the massage strength and execute the palm-rubbing movement; Record the experimental data; Repeat the force control experiment. Test seven groups of force data 10 times for each group, and calculate the average value. The third step in the experiment is to set up a constant massage force in the constant massage force control experiment.

In the control experiment of changing the massage force, the third step in the process of the experiment is to set a constant changing massage force within the range of 1~4 kg. The power of the electronic scale and the control power of the massage robot were collected and recorded in real-time by using the acquisition card.

#### B. MASSAGE POSITION TRACKING ACCURACY EXPERIMENT

##### 1) EXPERIMENTAL PRINCIPLES AND METHODS

The position of massage is one of the core factors affecting the curative effect of massage. The error of the robot tracking the massage position includes the identification and positioning error of the massage position, the conversion error between the robot space and the visual tracking space, and the motion error of the robot. In the paper, a motion platform was used to simulate the position and changes in different massage positions, and the recognition and tracking performance of the robot was tested.

The experimental platform consisted of a one-dimensional motion unit (including a one-dimensional motion platform, stepper motor driver and motion controller), binocular vision sensor, and target marker (fixedly connected with a one-dimensional motion platform). The massage robot recognizes

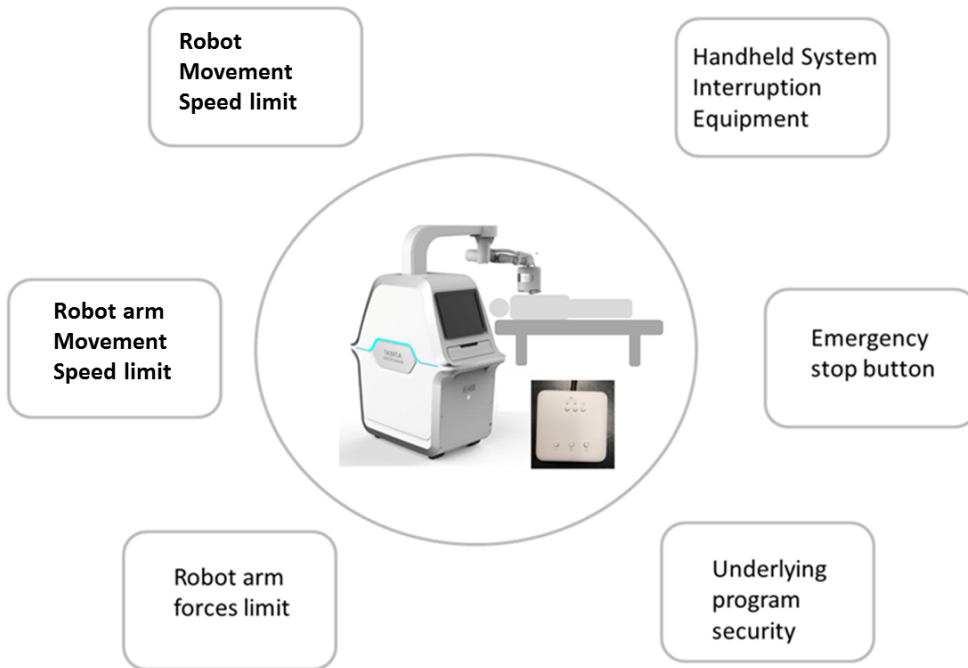


**FIGURE 2.** Security design.

and follows the motion of target marker points. The one-dimensional motion unit drives the target marker connected with it to move to a fixed position to simulate a massage position of the patient. After receiving the instruction, the robot recognizes the target marker and moves to the target marker point. The distance between the final position of the robot and the target marker point describes the accuracy of tracking the static massage position of the massage robot. When the one-dimensional motion element drives the fixed marker point to move, the robot tracks the moving trajectory of the target marker point in real-time. The real-time distance between the robot end position and the target marker point describes the accuracy of the massage robot tracking the dynamic massage position.

## 2) EXPERIMENTAL PROCESS

Experimental process for static position tracking of the massage position: Paste and fix the target marker on the one-dimensional motion mechanism; Control the movement of the one-dimensional platform to any point in the field of view; Start the visual program of the massage robot to track the motion trajectory of marker points; the tracking program records the deviation value calculated by each sampling; Process the deviation data after tracking stabilization.

Experimental process for dynamic position tracking of the massage position: Paste and fix the target marker on the one-dimensional motion mechanism; Control the movement of the one-dimensional platform to any point in the robot's field of view; Start the following program of the massage robot, follow the position of marker points, and wait for its stability; Control the one-dimensional movement platform to move

back and forth at a speed of 15 mm/s; The tracking program records the deviation of each sampling in each tracking process in real-time (the sampling frequency is 15 Hz).

## IV. THE PROPOSED TRUST ASSESSMENT FRAMEWORK, EXPERIMENT AND RESULTS ANALYSIS

The software and hardware safety test followed the international standard IEC 62304 and BG/BGIA risk assessment recommendations according to the machinery directive [28]–[31] with 8 hours uninterrupted operation and objective measurement.

### A. DESCRIPTION OF THE EMMA ROBOTIC SYSTEM

#### 1) MAINFRAME

The mainframe has an integrated robotic control system that includes the mechanical, electrical and software systems. The functions of the mainframe include the following: 1) it provides a screen interface that can assist physicians/users in accomplishing the setting of related programs; 2) users can use an external controller to control the motion of the robot, including conventional forward and backward movement as well as side to side and even rotation; and 3) it has a moving platform that can achieve rotational motion and up and down motion that can determine the spatial position of the robot arm.

#### 2) ROBOT ARM

A commercially available robot arm (Universal Robots UR3/CB3) is utilized and integrated into the EMMA robotic system. The main functions of the robot arm include the following: 1) assist human body recognition and position

identification before the massage procedure by positioning the camera to the required position; 2) execute massage motion according to the information from human body recognition; and 3) provide an emergency stop and retrieve function to ensure the safety of the patient.

### 3) MASSAGE END-EFFECTOR

The massage end-effector provides multiple massage manipulations to patients. It includes a finger massage manipulator, a palm massage manipulator, and a camera. Both the finger and the palm can achieve independent force control. In addition, there is a camera module that can capture and collect human body information and assist further massage manipulation. The general information about the function of the EMMA robot system is provided in Table 1.

### B. DESCRIPTION OF THE WORK TASK

Description of the operator's operations: The aim of the robot system is to minimize the operator's task, and thus, most of the treatment process has been automated. The operator must only select the region for the treatment process via the graphical user interface of the robot system, allowing the robot to plan out the course of the treatment. Once the planning is complete, the operator must initiate the treatment process, and the robot system will handle the rest. Description of the EMMA robot system's work activities: The robot system's main objective is to handle the treatment for the patient; once the operator has started the planning for the treatment process, the robot will plan the trajectories for the selected region. During the treatment, the robot arm will move the end-effector to the selected region and perform the massage operation depending on the type of treatment selected by the operator. Upon completion of the treatment, the robot arm will return to its rest position.

### C. HAZARD IDENTIFICATION AND RISK ASSESSMENT IN MASSAGE OPERATIONS

#### 1) DESCRIPTION

During the massage operation, physical contact between the robot system and an operator/patient can occur intentionally or unintentionally. The EMMA robot system is specifically designed for this particular type of operation. Risk reduction is achieved through inherently safe means in the robot and through a safety-related control system by keeping hazards associated with the robot system below threshold limit values that are determined during the risk assessment. A means to establish the threshold limits values are outlined in ISO/TS 15066-2016, Annex A. [32]

#### 2) CONTACT SITUATIONS

During the massage operation, contact events between the EMMA robot and body parts of the operator and patients come about in a number of ways:

**TABLE 1. EMMA robot system specification.**

Table 1 EMMA Robot System Specification

#### Mainframe

Dimensions: 1200\*1500\*500 mm

Weight: 250 kg

Reach: 650 mm

Lifting range: 150 mm

Lifting speed: 10 mm/s

Rotation range: 360 deg

Rotation speed: 3 rpm

Mobile base speed: 0.1 m/s

#### Robot arm

Weight: 11 kg

Payload: 3 kg

Reach: 500 mm

Degrees of freedom: 6 rotating joints

Speed: All wrist joints: 60 rpm  
Other joints: 180 rpm

#### End-effector

Dimensions: 180 x 160 x 200 mm

Weight: 3 kg

Force control range: 80 N

Force accuracy: ±5 N

Force control module speed: 50 mm/s

Finger rubbing coverage: Approx. 4.5 cm<sup>2</sup>

Finger rubbing speed: 80 rpm

Finger surface area: Approx. 1 cm<sup>2</sup>

Finger rubbing temperature: Approx. 40°C

Palm surface area: Approx. 50 cm<sup>2</sup>

Palm temperature: Approx. 40°C

#### Other

Programming The graphical user interface on 15-inch touchscreen

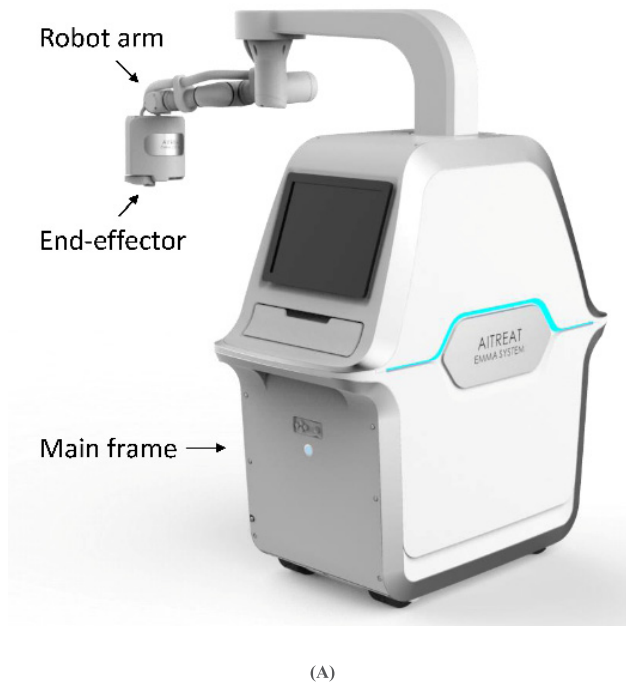
Noise: Comparatively noiseless

Power consumption: Approx. 300 watts using a typical program

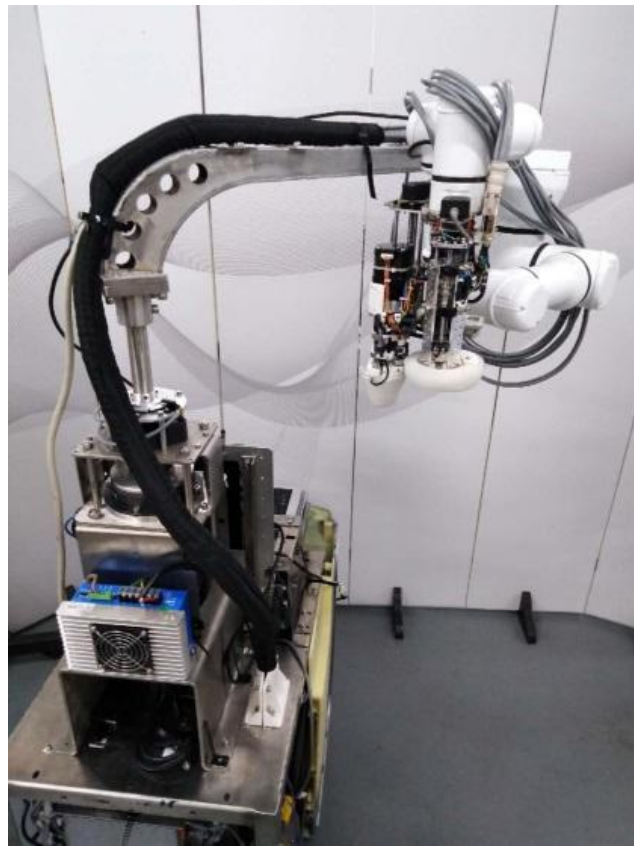
Materials: Stainless steel, Aluminum, PP plastic, Silicon

Power supply: 100-240 VAC, 50-60 Hz

Cabling: Power supply cable 1 m long



(A)



(B)

**FIGURE 3.** EMMA massage robot system.

Intended contact between the massage end-effector and the patient; Incidental contact situations, which can be a consequence of not following working procedures, but

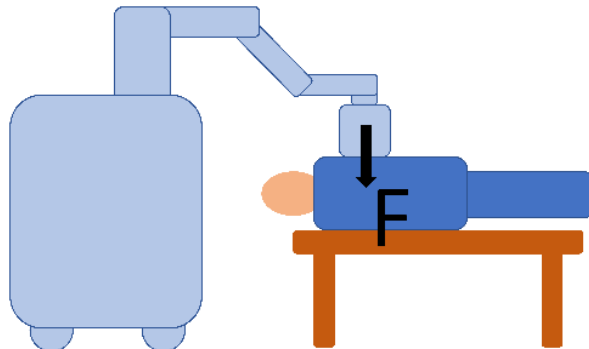
without a technical failure; Failure modes that lead to contact situations.

Possible types of contact between moving parts of the robot system and areas on a person's body are categorized in the following manner, as shown in Fig. 4.

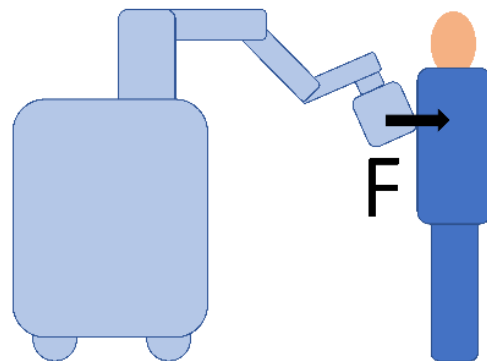
Quasi-static contact: this includes intentional massage treatment in which a person's body is limited between the massage end-effector and the bed, as shown in Fig. 4(a). In this situation, the robot would apply a pressure or force to the trapped body part for a time interval until the treatment is finished. Transient contact: as shown in Fig. 4(b), this is also referred to as "dynamic impact" and describes a situation in which a person's body part is impacted by a moving part of the robot system and can recoil or retract from the robot without clamping or trapping the contacted body area, thus making for a short duration of the actual contact.

### 3) PASSIVE AND ACTIVE RISK REDUCTION MEASURES

The EMMA robot system adopts both passive and active risk reduction measures to address quasi-static contact and transient contact. Passive safety design measures include the mechanical design of the robot system, whereas active safety design measures include the control design of the robot system.

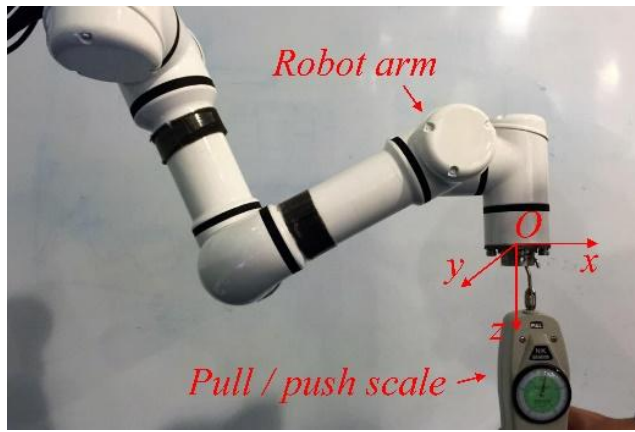


(A)

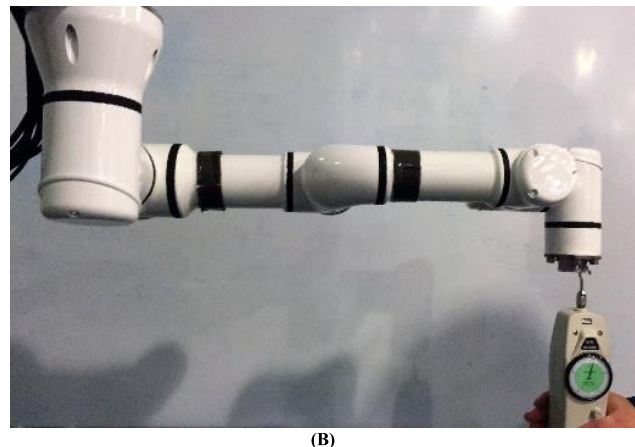


(B)

**FIGURE 4.** (A) Quasi-static contact, (B) transient contact.



(A)



(B)

**FIGURE 5.** External force testing of the robot arm, including (A) normal working configuration, and (B) extreme working condition.

#### a: PASSIVE SAFETY DESIGN METHODS

Passive safety design methods include the following:

Robot system surface design, including rounded edges and corners and smooth surfaces; compliant surfaces of silicon cover in the massage tools of the end-effector; Energy absorbing unit within the force-control module of the massage end-effector.

#### b: ACTIVE SAFETY DESIGN METHODS

Active safety function from the robot arm: The robot arm is a commercially available robot arm (Universal Robots UR3/CB3) that has related certifications regarding the safety of collaborative operation. Maximum velocity of the robot arm: Through the program, we set the velocity limit of the robot arm to 0.62 m/s in the massage operation (maximum of 1 m/s). The maximum force of the robot arm: We have conducted an experiment to check the maximum external force the robot arm can withstand (generate). The detail of the experiment was included in paragraph 4. From the experiment, we can identify the maximum external force

**TABLE 2.** External force to trigger the protective stop of the robot arm.

Configuration	Force value (N)				
	+z	-z	+x	-x	-y
Normal	150	150	132	150	160
Extreme	110	95	105	100	150

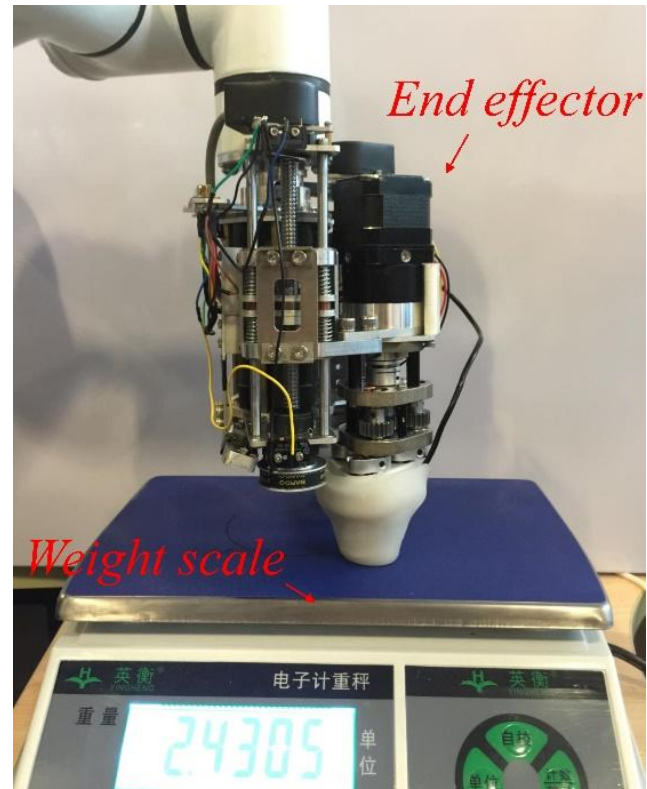


**FIGURE 6.** Force calibration setup of the finger force control module.

that the robot arm can withstand in the normal massage configuration and in the extreme configuration. Use of the safety-rated monitored stop function: UR3 has an emergency stop button embedded in the teaching pendant, which can stop the motion of the robot arm; UR3 has a safety-related control system which enables protective stoppage when it experiences external hazards.

Active safety function from the massage end-effector: Maximum velocity of the end-effector: The maximum velocity of the end-effector force control motion is set to be 50 mm/s. The maximum force of the end-effector: We have conducted force calibration of the massage end-effector in terms of both finger force control and palm force control. Paragraph 5 gives the details of the force calibration procedure, and the result shows the calibration results of both finger and palm force control modules. These data were utilized to establish the force control of the massage and safety-rated monitored stop function. Use of the safety-rated monitored stop function: The patient has a remote controller, which can

**TABLE 3.** Risk assessment of physical contact during the massage operation.

Contact situation	Contact type*	Exposed body region	Frequency of occurrence	Permissible biomechanical limit(s)	Risk reduction measures
Normal massage treatment	1) intended contact; 2) quasi-static contact	Back and shoulders	high	Back and shoulders: 210 N	1) passive methods: 2) active methods: end-effector limits massage force to 60 N
End-effector functions incorrectly	1) failure mode; 2) quasi-static contact	Back and shoulders	low	Back and shoulders: 210 N	1) passive methods: 2) active methods: robot arm will be protectively stopped around 100 - 150 N
Robot arm too close to human body	1) failure mode; 2) quasi-static contact	Back and shoulders	medium	Back and shoulders: 210 N	1) passive methods: 2) active methods: robot arm will be protectively stopped around 100 - 150 N
Robot presses incorrect body regions	1) failure mode; 2) quasi-static contact	Neck, back and shoulders	medium	Neck: 150 N Back and shoulders: 210 N	1) passive methods: 2) active methods: end-effector limits massage force to 60 N
Collision between human and robot	1) incidental contact; 2) transient contact	Chest, neck, back and shoulders	low	Head: 0.23 J Neck: 0.84 J Chest: 1.6 J Back and shoulders: 2.5 J	Transfer energy calculated**: Head: 0.15 J Neck: 0.04 J Chest: 0.4 J Back and shoulders: 0.4 J

\* In quasi-static-type contact, the pressing force is selected to represent the permissible biomechanical limit, while in transient-type contact, the transfer energy is selected instead (ISO/TS 15066-2016, Annex A).

\*\* Transfer energy is calculated according to the transient contact equations in ISO/TS 15066-2016, Annex A, where the effective mass of the robot is 10 kg, the effective mass of the human body region is selected from Table A.3, and the relative speed is 0.1 m/s.

increase and decrease force and emergently retrieve the end-effector and robot arm.

In addition, the end-effector contains an embedded encoder to monitor the contact speed and force sensor to monitor contact force during the massage operation.

#### D. TESTING OF THE MAXIMUM EXTERNAL FORCE THE ROBOT ARM CAN WITHSTAND

An experimental test was conducted to test the maximum external force the robot arm can withstand. The purpose of this experiment was to identify how much force the robot arm can apply to the human body. Generally, the capability of resisting external force is based on the position of the robot arm, without loss of generality, and two typical configurations of the robot arm are selected, including a normal working

configuration and an extreme working configuration. These two configurations are shown in Fig. 5. For each configuration, a push/pull scale was utilized to apply both push and pull force to the end-effector of the robot arm. Furthermore, a coordinate frame {O-xyz} is attached at the center of the end-effector, with the +z perpendicular to the end-effector plane, the +x axis along the intersection line of the end-effector plane and the robot arm plane, and the +y axis following the right-hand rule. Pulling force is applied along the +x, +y, and +z axes, and pushing force is vice versa (only the y-axis force was tested due to the symmetry of the robot arm configuration). In each case, we gradually increase the pushing/pulling force and record the value at which the robot arm appears to protectively stop. The testing result is presented in Table 2.

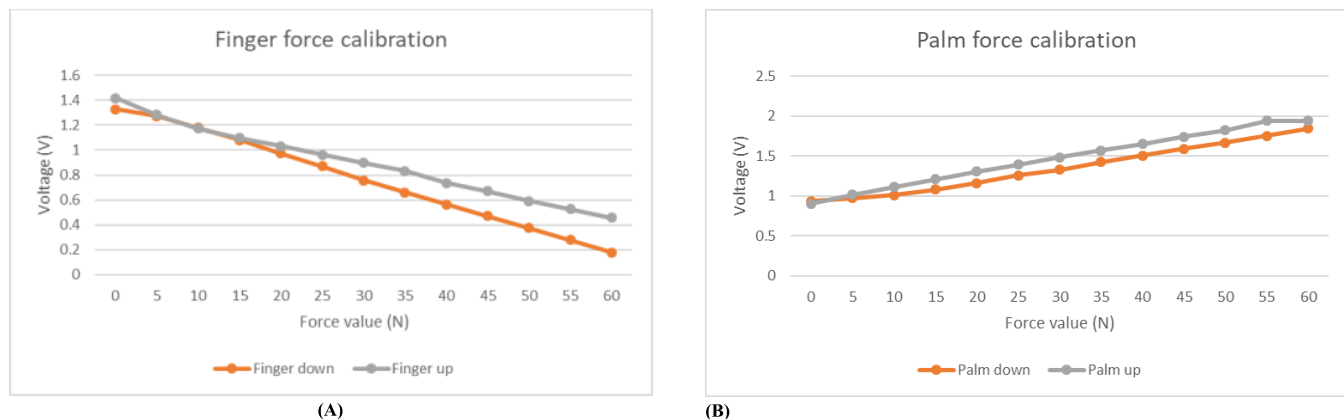


**FIGURE 7.** Force calibration of the EMMA massage end-effector, including the finger force calibration (A) with a maximum force 100 N and the palm force calibration (B) with a maximum force 60 N. The x-axis represents the force value, and the y-axis represents the voltage value.

### E. FORCE CALIBRATION OF THE MASSAGE END-EFFECTOR

Force calibration of the massage end-effector was conducted to establish the relationship between the force the end-effector applies to the environment and the voltage of the sensor embedded in the force-control module. The force calibrations of both the finger and palm module have been conducted, and Fig. 6 shows the calibration setup of the finger force control module. The calibration results were further recorded and presented in Fig. 6. In particular, finger force up to 100 N and palm force up to 60 N were recorded. These values were utilized to conduct force feedback control of the massage end-effector as well as setup the safety function of the handheld device.

### F. RISK ASSESSMENT OF PHYSICAL CONTACT DURING THE MASSAGE OPERATION

See Table 3.

### V. CONCLUSIONS, DISCUSSION, AND OUTLOOK

In this paper, according to a series of test research programs, we obtained the confirmation of Reliability and safety to the EMMA massage robot, by means of the realistic based test, the EMMA massage robot safety automatic control is effective; and the protection strategy and design measures had been implemented. In particular, it should be noted that the handheld system interruption equipment achieved the design goal, it achieved effective interruptions and protection during the testing. From a device design perspective, the EMMA massage robot is ready to conduct clinical trials for healthy volunteers.

This safety test and report is the first step for the EMMA Massage Robot, and its automatic diagnosis, which is based on data mining and brain-based networks, and therapy plan design are the next development directions. The brain-based model networks have gradually been considered more popular than deep learning networks after the year 2001 [33], due to a large number of studies in the brain sciences that have shown that the human brain network is not a cascade structure [34], [35]. Therefore, massage robot therapists

with an independent judgment can be effective assistants to clinical doctors or therapists with much IoT repetitive work. However, all functions must follow the safe and harmless basic principle. In this study, all tested force, robot and robot arm movement, current intensity, etc., are within the human acceptable limits, which are far from dangerous edge values [20], [36], [37].

The next phase will develop the functions of precise force quantitative treatment and precise pressure-controlled cupping therapy, all of which are based on the safety principles that have been tested, to prepare for further study and clinical trials. With the increase in the number of patients and the accumulation of data, brain-based networks and data mining will allow the EMMA Massage Robot to show the advantages of data integration capabilities [38]–[45]. Through treatment effect feedback by data input and sensor detection, it will become an experienced clinician, which no human clinician can match because of life and time limits.

### ACKNOWLEDGMENT

The authors would like to thank the code engineers working behind the scenes, as well as our cooperation mechanical manufacturer in Shenzhen, China, for doing so much for the EMMA massage robot and the test project. They would also like to thank the professional experts at NTU who advised our team; their ideas provided us with IoT inspiration.

### REFERENCES

- [1] IEC. *International IEC Standard-International Electrotechnical Commission*. Accessed: Jun. 2, 2012. [Online]. Available: <https://ihsmarkit.com/products/iec-standards.html>
- [2] US Department Health Human Services. *Recognized Consensus Standards, FDA US Food and Drug Administration*. Accessed: Aug. 20, 2012. [Online]. Available: <https://healthdata.gov/dataset/fda-recognized-consensus-standards>
- [3] K. Hall. (Jun. 1, 2010). Developing medical device software to IEC 62304. EMDT-European Medical Device Technology. Accessed: Dec. 11, 2012. [Online]. Available: <https://www.smtcorp.com/drupal/ext/www.emdt.co.uk/index.html>
- [4] EUR-Lex-31993L0068-EN. Accessed: Sep. 7, 2015. [Online]. Available: <https://www.Eur-lex.europa.eu>

- [5] *CE Marking*. Accessed: Feb. 2017. [Online]. Available: [https://en.wikipedia.org/wiki/CE\\_marking](https://en.wikipedia.org/wiki/CE_marking)
- [6] R. Buyya and A. V. Dastjerdi, *Internet of Things: Principles and Paradigms*, 1st ed. San Mateo, CA, USA: Morgan Kaufmann, 2016.
- [7] S. Deng, L. Huang, J. Taheri, J. Yin, M. Zhou, and A. Y. Zomaya, “Mobility-aware service composition in mobile communities,” *IEEE Trans. Syst., Man, Cybern., Syst.*, vol. 47, no. 3, pp. 555–568, Mar. 2017.
- [8] S. Deng, H. Wu, W. Tan, Z. Xiang, and Z. Wu, “Mobile service selection for composition: An energy consumption perspective,” *IEEE Trans. Autom. Sci. Eng.*, vol. 14, no. 3, pp. 1478–1490, Jul. 2017.
- [9] D. Mewes and F. Mauser, “Safeguarding crushing points by limitation of forces,” *Int. J. Occupational Saf. Ergonom.*, vol. 9, no. 2, pp. 177–191, 2003.
- [10] K. Saita, Y. Yamada, N. Tsuchida, K. Imai, H. Ikeda, and N. Sugimoto, “A failure-to-safety ‘Kyozon’ system with simple contact detection and stop capabilities for safe human-autonomous robot coexistence,” in *Proc. IEEE Int. Conf. Robot. Autom.*, Nagoya, Japan, vol. 3, May 1995, pp. 3089–3096.
- [11] Y. Chen, S. Deng, J. Yin, and H. Ma, “Deploying data-intensive applications with multiple services components on edge,” in *Mobile Networks and Applications*. 2019. doi: [10.1007/s11036-019-01245-3](https://doi.org/10.1007/s11036-019-01245-3).
- [12] J. Yu, C. Hong, Y. Rui, and D. Tao, “Multitask autoencoder model for recovering human poses,” *IEEE Trans. Ind. Electron.*, vol. 65, no. 6, pp. 5060–5068, Jun. 2018.
- [13] H. Gao, Y. Duan, H. Miao, and Y. Yin, “An approach to data consistency checking for the dynamic replacement of service process,” *IEEE Access*, vol. 5, pp. 11700–11711, 2017.
- [14] J. Weng, J. McClelland, A. Pentland, O. Sporns, I. Stockman, M. Sur, and E. Thelen, “Autonomous mental development by robots and animals,” *Science*, vol. 291, no. 5504, pp. 599–600, Jan. 2001.
- [15] Y. Yin, L. Chen, Y. Xu, and J. Wan, “Location-aware service recommendation with enhanced probabilistic matrix factorization,” *IEEE Access*, vol. 6, pp. 62815–62825, 2018.
- [16] S. Liu, Z. Pan, and X. Cheng, “A novel fast fractal image compression method based on distance clustering in high dimensional sphere surface,” *Fractals*, vol. 25, no. 4, Aug. 2017, Art. no. 1740004.
- [17] Y. Yin, F. Yu, Y. Xu, L. Yu, and J. Mu, “Network location-aware service recommendation with random walk in cyber-physical systems,” *Sensors*, vol. 17, no. 9, p. 2059, Sep. 2017.
- [18] H. Gao, H. Miao, L. Liu, J. Kai, and K. Zhao, “Automated quantitative verification for service-based system design: A visualization transform tool perspective,” *Int. J. Softw. Eng. Knowl. Eng.*, vol. 28, no. 10, pp. 1369–1397, 2018.
- [19] Q. Peng, M. Zhou, Q. He, Y. Xia, C. Wu, and S. Deng, “Multi-objective optimization for location prediction of mobile devices in sensor-based applications,” *IEEE Access*, vol. 6, pp. 77123–77132, 2018.
- [20] H. Gao, D. Chu, Y. Yin, and Y. Duan, “Probabilistic model checking-based service selection method for business process modeling,” *J. Softw. Eng. Knowl. Eng.*, vol. 27, no. 6, pp. 897–923, 2017.
- [21] J. Weng, “Brains as naturally emerging turing machines,” in *Proc. Int. Joint Conf. Neural Netw.*, Killarney, Ireland, Jul. 2015, pp. 1–8.
- [22] S. Lou, G. Srivastava, and S. Liu, “A node density control learning method for the Internet of Things,” *Sensors*, vol. 19, no. 15, p. 3428, 2019.
- [23] R. M. Alexander, “Mechanics of animal movement,” *Current Biol.* vol. 15, no. 16, pp. R616–R619, Aug. 2005. doi: [10.1016/j.cub.2005.08.016](https://doi.org/10.1016/j.cub.2005.08.016).
- [24] H. Hatze, “Letter: The meaning of the term ‘biomechanics,’” *J. Biomech.*, vol. 7, no. 2, pp. 189–190, Mar. 1974. doi: [10.1016/0021-9290\(74\)90060-8](https://doi.org/10.1016/0021-9290(74)90060-8).
- [25] H. Gao, W. Huang, X. Yang, Y. Duan, and Y. Yin, “Toward service selection for workflow reconfiguration: An interface-based computing solution,” *Future Gener. Comput. Syst.*, vol. 87, pp. 298–311, Oct. 2018.
- [26] Y. Yin, F. Yu, Y. Xu, L. Yu, and J. Mu, “Network location-aware service recommendation with random walk in cyber-physical systems,” *Sensors* vol. 17, no. 9, p. 2059, Sep. 2017.
- [27] H. Gao, K. Zhang, J. Yang, F. Wu, and H. Liu, “Applying improved particle swarm optimization for dynamic service composition focusing on quality of service evaluations under hybrid networks,” *Int. J. Distrib. Sensor Netw.*, vol. 14, no. 2, Feb. 2018, Art. no. 1550147718761583.
- [28] S. Deng, Z. Xiang, J. Yin, J. Taheri, and A. Y. Zomaya, “Composition-driven IoT service provisioning in distributed edges,” *IEEE Access*, vol. 6, pp. 54258–54269, 2018.
- [29] G. Srivastava, A. Fisher, R. Bryce, and J. Crichigno, “Green communication protocol with geolocation,” in *Proc. IEEE 89th Veh. Technol. Conf.*, Kuala Lumpur, Malaysia, Apr./May 2019, pp. 1–6. doi: [10.1109/VTCpring.2019.8746376](https://doi.org/10.1109/VTCpring.2019.8746376).
- [30] Y. Yin, Y. Xu, W. Xu, M. Gao, L. Yu, and Y. Pei, “Collaborative service selection via ensemble learning in mixed mobile network environments,” *Entropy*, vol. 19, no. 7, p. 358, 2017.
- [31] *Robots and Robotic Devices—Safety Requirements for Industrial Robots—Part 1: Robots*, Standard ISO/TS 15066, 2016.
- [32] C. Zhang, S. Deng, and H. Zhao, “A density-based offloading strategy for IoT devices in edge computing systems,” *IEEE Access* vol. 6, pp. 73520–73530, 2018.
- [33] S. Deng, L. Huang, D. Hu, J. L. Zhao, and Z. Wu, “Mobility-enabled service selection for composite services,” *IEEE Trans. Services Comput.*, vol. 9, no. 3, pp. 394–407, May/Jun. 2016.
- [34] S. Liu, W. Bai, G. Liu, W. Li, and H. M. Srivastava, “Parallel fractal compression method for big video data,” *Complexity*, vol. 2018, Oct. 2018, Art. no. 2016976. doi: [10.1155/2018/2016976](https://doi.org/10.1155/2018/2016976).
- [35] Deutsche Gesetzliche Unfallversicherung. (Oct. 2006). *BG/BGIA Risk Assessment Recommendations According to Machinery Directive, Design of Workplaces With Collaborative Robots*. Accessed: Feb. 2011. [Online]. Available: [http://publikationen.dguv.de/dguv/pdf/10002/bg\\_bgia\\_empf\\_u\\_001e.pdf](http://publikationen.dguv.de/dguv/pdf/10002/bg_bgia_empf_u_001e.pdf)
- [36] C.-G. Kang, B.-J. Lee, I.-X. Son, and H.-Y. Kim, “Design of a percussive massage robot tapping human backs,” in *Proc. IEEE Int. Symp. Robot Hum. Interact. Commun.*, Aug. 2007, pp. 962–967.
- [37] S. Liu, W. Fu, L. He, J. Zhou, and M. Ma, “Distribution of primary additional errors in fractal encoding method,” *Multimedia Tools Appl.*, vol. 76, no. 4, pp. 5787–5802, Feb. 2017.
- [38] Z. Zhou, J. Feng, B. Gu, B. Ai, S. Mumtaz, J. Rodriguez, and M. Guizani, “When mobile crowd sensing meets UAV: Energy-efficient task assignment and route planning,” *IEEE Trans. Commun.*, vol. 66, no. 11, pp. 5526–5538, Nov. 2018.
- [39] Z. Zhou, M. Dong, K. Ota, G. Wang, and L. T. Yang, “Energy-efficient resource allocation for D2D communications underlaying cloud-RAN-based LTE-A networks,” *IEEE Internet Things J.*, vol. 3, no. 3, pp. 428–438, Jun. 2016.
- [40] Z. Zhou, J. Gong, Y. He, and Y. Zhang, “Software defined machine-to-machine communication for smart energy management,” *IEEE Commun. Mag.*, vol. 55, no. 10, pp. 52–60, Oct. 2017.
- [41] Z. Zhou, H. Liao, B. Gu, K. M. S. Huq, S. Mumtaz, and J. Rodriguez, “Robust mobile crowd sensing: When deep learning meets edge computing,” *IEEE Netw.*, vol. 32, no. 4, pp. 54–60, Jul./Aug. 2018.
- [42] X. Lin, J. Li, J. Wu, H. Liang, and W. Yang, “Making knowledge tradable in edge-AI enabled IoT: A consortium blockchain-based efficient and incentive approach,” *IEEE Trans. Ind. Informat.*, to be published. doi: [10.1109/TII.2019.2917307](https://doi.org/10.1109/TII.2019.2917307).
- [43] G. Li, J. Wu, J. Li, K. Wang, and T. Ye, “Service popularity-based smart resources partitioning for fog computing-enabled industrial Internet of things,” *IEEE Trans. Ind. Informat.*, vol. 14, no. 10, pp. 4702–4711, Oct. 2018.
- [44] A. D. Dwivedi, L. Malina, P. Dzurenda, and G. Srivastava, “Optimized blockchain model for Internet of Things based healthcare applications,” 2019, *arXiv:1906.06517*. [Online]. Available: <https://arxiv.org/abs/1906.06517>
- [45] A. D. Dwivedi, P. Morawiecki, and G. Srivastava, “Differential cryptanalysis of round-reduced speck suitable for Internet of Things devices,” *IEEE Access*, vol. 7, pp. 16476–16486, 2019.



**WEN SI** was a Postdoctoral Research Associate with Rehabilitation Medicine in Huashan Hospital, Fudan University. He is currently an Associate Professor with the Internet of Things (IoT) Engineering Department, Shanghai Business School. His research interest areas include biomedical engineering and the IoT technologies. His experience is mainly focused on a technical scheme for human motion detection, including the tri-axial force on the foot-ground interface and human body modeling of movement and may enhance the effect of recovery training.



**GAUTAM SRIVASTAVA** received the B.Sc. degree from Briar Cliff University, USA, in 2004, and the M.Sc. and Ph.D. degrees from the University of Victoria, Victoria, BC, Canada, in 2006 and 2012, respectively. He then taught for three years at the Department of Computer Science, University of Victoria, where he was regarded as one of the top undergraduate professors in the Computer Science Course Instruction. In 2014, he joined a tenure-track position at Brandon University, Brandon, MB, Canada, where he is currently active in various professional and scholarly activities. He was promoted to the rank of Associate Professor, in January 2018. As he is popularly known, he is active in research in the field of cryptography, data mining, security and privacy, and blockchain technology. In his five years as a Research Academic, he has published a total of 45 articles in high-impact conferences in many countries and in high-status journals (SCI and SCIE) and has also delivered invited guest lectures on big data, cloud computing, the Internet of Things, and cryptography at many universities worldwide. He is also active in research projects with other academics in Taiwan, Singapore, Canada, Czech Republic, Poland, and USA. He is an Editor for several SCI/SCIE journals. He is an Associate Editor of the world-renowned IEEE ACCESS journal.



**YIZHONG ZHANG** received the B.S. degree in biomedical science and the M.D. degree in traditional Chinese medicine from Nanyang Technological University, Singapore, in 2010. He has been a Singapore Registered Chinese Physician, since 2011, and invented the EMMA robotic massage system, in 2013. His research interests include clinical studies in integrative medicine of physical therapy and Chinese medicine for degenerative diseases and pain management. He is an Editor of the journal of the Academy of Chinese Medicine, Singapore.



**LEI JIANG** graduated from the Heilongjiang Medical University of TCM and from the Software College, East China Normal University. He is currently pursuing the Ph.D. degree. He participated in medical equipment and software development projects as a Clinical Doctor-Software Engineer. He has been with the clinic as a TCM Doctor, since 2006. Since 2012, he has also been with the Hannover Medical School, where he focuses on integrated Chinese medicine research and medical equipment development, which relates closely to Chinese medicine. He is a Specialist in traditional Chinese medicine (TCM) and software engineering. He is also a Senior Clinical Doctor and Researcher. He is a Peer Reviewer of many professional journals both in medical and software engineering fields, such as functional nuclear magnetic resonance (fMRI), diffusion tensor imaging (DTI), Chinese medical skill, acupuncture, Tuina therapy, Chinese herbal medicine, physical medicine, and rehabilitation medicine, as well as software, automated control, machine learning, and data mining.

• • •